Science of the Total Environment 899 (2023) 165665

Contents lists available at ScienceDirect

Science of the Total Environment

journal homepage: www.elsevier.com/locate/scitotenv

# Vegetation restoration altered the soil organic carbon composition and favoured its stability in a *Robinia pseudoacacia* plantation

Zhuoxia Su [a], Yangquanwei Zhong [b], Xiaoyue Zhu [a], Yang Wu [a], Zhifeng Shen [c], Zhouping Shangguan [a,*]

[a] State Key Laboratory of Soil Erosion and Dryland Farming on the Loess Plateau, Northwest A & F University, Yangling, Shaanxi 712100, China
[b] School of Ecology and Environment, Northwestern Polytechnical University, Xi'an 710072, China
[c] Henan University, Kaifeng 475004, China

ARTICLE INFO

Editor: Manuel Esteban Lucas-Borja

*Keywords:*
Lignin phenols
Microbial necromass
Organic carbon fractions
Nuclear magnetic resonance
Soil organic carbon stabilization

ABSTRACT

Soil organic carbon (SOC) stabilization is vital for the mitigation of global climate change and retention of soil carbon stocks. However, there are knowledge gaps on how SOC sources and stabilization respond to vegetation restoration. Therefore, we investigated lignin phenol and amino sugar biomarkers, SOC physical fractions and chemical structure in one farmland and four stands of a *Robinia pseudoacacia* plantation. We observed that the content of SOC increased with afforestation, but the different biomarkers had different contributions to SOC. Compared to farmland, the contribution of lignin phenols to SOC decreased in the plantations, whereas there was no difference among the four stand ages, likely resulting from the balance between increasing lignin derivation input and increasing lignin degradation. Conversely, vegetation restoration increased the content of microbial necromass carbon (MNC) and the contribution of MNC to SOC, mainly because microbial residue decomposition was inhibited by decreasing the activity of leucine aminopeptidase, while microbial necromass preservation was promoted by adjusting soil variables (soil water content, clay, pH and total nitrogen). In addition, vegetation restoration increased the particulate organic carbon (POC), mineral-associated organic carbon (MAOC) pools and the O-alkyl C intensify. Overall, vegetation restoration affected SOC composition by regulating lignin phenols and microbial necromass and also altered SOC stabilization by increasing the physically stable MAOC pool during late afforestation. The results of this study suggest that more attention should be given to SOC sequestration and stability during late vegetation restoration.

## 1. Introduction

Global carbon dioxide ($CO_2$) levels in 2019 have been at their highest for at least 2 million years (IPCC, 2021). Therefore, global warming has become one of the most urgent ecological and environmental issues facing all mankind (IPCC, 2021) and may affect soil ecological functions such as carbon sequestration and structural stability (Lal, 2004b). It has been reported that soil contains 1500–2400 Gt C, which is 3–4 times that of the vegetation carbon pool and 2–3 times that of the atmosphere carbon pool (Friedlingstein et al., 2020). Small variations of global SOC stock may therefore affect the global $CO_2$ concentration (Lal, 2004a; Bradford et al., 2016). Researchers have attempted to reduce $CO_2$ emissions and increase carbon sequestration in soil through vegetation restoration (Deng et al., 2017). However, we lack sufficient capacity to forecast changes in the SOC pools and how they will respond to revegetation. This is largely because our understanding of the process of SOC formation and stabilization remains poor.

Soil organic matter is composed of a series of organic compounds from plants and microorganisms at different decomposition stages (Lehmann and Kleber, 2015). Traditionally, plant structural compounds (such as lignin) were considered the main contributor to the slow-cycling SOC pool due to their chemical recalcitrance (Thevenot et al., 2010). The emerging view focuses on the role of microorganisms in mediating SOC formation. Liang et al. (2017) proposed a conceptual framework regarding the "microbial carbon pump", which underlined the crucial effect of microbial anabolism on regulating the carbon cycle. Plant-derived carbon can be changed into microbial-derived carbon via two microbial metabolic pathways: ex vivo modification and in vivo turnover (Liang et al., 2017; Zhu et al., 2020; Whalen et al., 2022). Then, microbial residues are further enclosed in aggregates (entombing effect)

* Corresponding author at: Xinong Rd. 26, Institute of Soil and Water Conservation, Yangling, Shaanxi 712100, China.
*E-mail address:* shangguan@ms.iswc.ac.cn (Z. Shangguan).

https://doi.org/10.1016/j.scitotenv.2023.165665
Received 20 April 2023; Received in revised form 17 July 2023; Accepted 18 July 2023
Available online 19 July 2023

or combined with mineral particles, which are conducive to the formation of a stable SOC pool (Chen et al., 2020; Liang, 2020). Lignin phenol and amino sugar, as two specific biomarkers, have been extensively used to indicate plant-derived and microbial-derived carbon. Some studies exploring the impact of forest conversion/reforestation on microbial necromass accumulation have reported divergent results, with positive (Shao et al., 2019; Li et al., 2022b; Li et al., 2023), insignificant or negative (Ma et al., 2022). These differences may be attributed to differences in climate regions, and biotic and abiotic factors. Hence, it is essential to explore the distribution differences of plant-derived carbon and microbial-derived carbon during the afforestation process, as well as their effect on SOC pool formation and accumulation.

The stability of SOC was correlated with long-lasting SOC sequestration (Mustafa et al., 2022). At present, SOC physical fractions combined with chemical structure have been used to evaluate SOC stability (Mustafa et al., 2022). Generally, SOC is separated into coarse particulate organic carbon (cPOC), fine particulate organic carbon (fPOC) and mineral-associated organic carbon (MAOC) (Gill et al., 1999). Particulate organic carbon (POC) and MAOC are different in source and turnover. POC is primarily composed of partially decomposed plant residues, whereas MAOC is derived from microbial necromass and products and adsorbed by soil minerals (Yu et al., 2022). In addition, MAOC decomposed slower than POC and was retained in the soil for long periods. Thus, it represents a pivotal carbon pool for persistent SOC sequestration (Lavallee et al., 2019; Yu et al., 2022). Nuclear magnetic resonance (NMR) spectroscopy is an effective technique to evaluate the composition of functional groups and SOC chemical stability (Yang et al., 2022a). Alkyl-C originates from plant cutin and waxes and is considered the most persistent part of stable organic matter (Wu et al., 2016). Conversely, O-alkyl C is regarded as liable organic matter rich in carbohydrate compounds (Mo et al., 2022). Therefore, the combination of physical fractions and chemical structure is helpful to completely understand SOC stability during afforestation.

Owing to its low vegetation coverage rate and serious soil erosion, the Loess Plateau is one of the most ecologically fragile places in China and the world (Deng et al., 2016). As a major means of soil restoration in fragile habitats, vegetation restoration is a main factor influencing soil organic carbon and its accumulation (Deng et al., 2014). Since 1950, numerous strategies have been launched by the government to restore deteriorating ecological environments; moreover, the 'Grain for Green' program was carried out in 1999 to restore fragile ecosystems (Fu et al., 2017), which have an active part in regional carbon sequestration and even carbon balance worldwide. Vegetation restoration is also important for regulating the $CO_2$ content in the atmosphere, realizing soil carbon neutrality. Nevertheless, there is very little information about how vegetation restoration regulates SOC formation, turnover and stabilization. Therefore, we investigated farmland and four *Robinia pseudoacacia* plantations aged 15 to 45 years to explore (1) how vegetation restoration affects plant-derived SOC and microbial-derived SOC accumulation and their contributions to SOC and (2) how afforestation influences different soil SOC fractions and stability. We hypothesized that (1) vegetation restoration increases litter input (Zhang et al., 2019), which promotes plant-derived carbon content; (2) vegetation restoration promotes necromass C accumulation and its contribution to SOC by inhibiting necromass C decomposition and increasing necromass C preservation; and (3) vegetation restoration alters SOC stability by increasing the stable MAOC pool.

## 2. Materials and methods

### 2.1. Study area and sample collecting

We conducted the study in the Huaiping Forest Farm of Yongshou County (34°50′8″–34°50′39″N, 108°04′52″–108°05′11″E), Shaanxi Province, in the southern part of the Loess Plateau, China (Fig. 1). This area belongs to the temperate subhumid climate zone. The mean annual temperature is 10.8 °C. The average annual precipitation is 605 mm, of which over 60 % falls from July to September (Liu et al., 2017). The soil is Calcaric Regosols in the WRB soil classification (Liu et al., 2022a). The elevation is 1123–1464 m. The government of Yongshou County has taken effective measures to reduce water and soil erosion since 1951, such as forbidding deforestation, fencing natural forests, and converting cropland to plantations (Liu et al., 2020). The main crop types before afforestation were wheat and maize (Liu et al., 2018). Currently, this area contains a large number of *R. pseudoacacia* artificial forests, which account for approximately 85 % of the afforestation area. There are also a few *Pinus tabulaeformis* and *Platycladus orientalis* artificial forests. The vegetation grows well in this study area, and the dominant shrubs contain *Lespedeza floribunda*, *Rosa davurica*, etc. The grass species under the crown consist of *Aster ageratoides*, *Rubus parvifolius*, *Chenopodium album, Artemisia argyi*, etc.

Based on well-documented literature, local elders and field

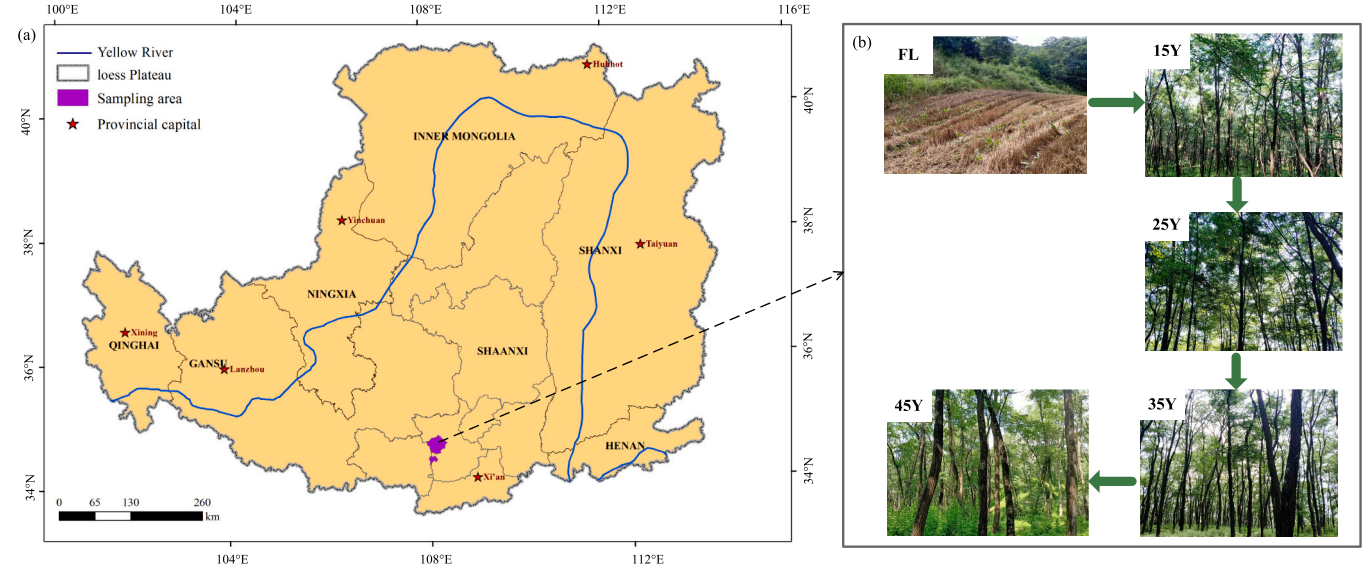


**Fig. 1.** The location map of the study area and specific photos of the different sites. FL: farmland, 15Y: 15-year-old forestland; 25Y: 25-year-old forestland; 35Y: 35-year-old forestland; 45Y: 45-year-old forestland.

investigations, a chronosequence including four age classes (15, 25, 35, and 45 years) of *R. pseudoacacia* plantations and one farmland was selected in our study (Fig. 1). Table S1 illustrates the sampling site information regarding the location, slope degree and vegetation characteristics. At each restoration site and the farmland, we randomly set three 20 m × 20 m separate plots in July 2020. In total, 15 plots (5 ages × 3 replicate plots) were established in the experimental field. Before soil sampling, we measured the traits of *R. pseudoacacia*, such as crown breadth (CB) and diameter at breast height (DBH). Furthermore, we randomly established three 1 m × 1 m squares in each plot to investigate the understory species. Aboveground vegetation in each square was collected by the cutting method and dried to constant weight in an oven to calculate aboveground biomass (AGB). After removing litter and dead wood from each square, we collected soil using a soil auger from the topsoil layer (0–20 cm) in a "S" shape. Then, we removed small stones and plant and animal debris from the soil and passed it through a 2-mm mesh. Subsequently, soil samples were divided into three subsamples: one was immediately stored at 4 °C for the determination of soil extracellular enzyme activities, the second was stored at −80 °C to measure soil microbial phospholipid fatty acids (PLFAs), and the third was air-dried at room temperature for further determination and analysis.

### 2.2. Soil property analyses

The SOC was oxidized using $H_2SO_4$-$K_2Cr_2O_7$ and oil-boiling and then titrated by $FeSO_4$ solution. Soil easily oxidized carbon (EOC) was extracted by 333 mmol/L $KMnO_4$ and then assayed by a spectrophotometer (Blair et al., 1995). Soil microbial biomass carbon and nitrogen (MBC and MBN) were first analyzed by chloroform fumigation and then measured by a TOC analyzer (Brookes et al., 1985; Vance et al., 1987). The soil dissolved organic carbon (DOC) and nitrogen (DON) were expressed without the chloroform fumigated part. We also analyzed the soil total nitrogen (STN), ammonium nitrogen (AN), nitrate nitrogen (NN), soil total phosphorus (STP), available phosphorus (SAP) concentrations. Soil physical properties such as bulk density (BD), particle composition (clay, silt and sand), soil water content (SWC) and soil pH were assayed according to standard analytical procedures. The descriptions of these methods are shown in Supplementary Method S1.

### 2.3. PLFAs and enzymatic activities

The soil microbial PLFAs were analyzed by a gas chromatograph (GC) (Agilent 7890A). In short, approximately 3 g freeze-dried soil was extracted, fractionated, and purified according to Yuan et al. (2016). A mixture consisting of citrate buffer, chloroform and methanol (0.8:1:2 v/v/v) was used to conduct the extraction. Then, phospholipids were separated on a silica acid column, followed by alkaline methanolysis to their fatty acid methyl esters (FAMEs). The internal standard of methyl nonadecanoate fatty acid (19:0) was used to quantify the phospholipid concentrations. The identification of microbes (gram-positive bacteria (GP), gram-negative bacteria (GN), fungi, and actinomycete groups) of specific PLFAs is shown in Table S2.

We measured C-acquiring enzymes (BG; β-1,4-glucosidase, CBH; cellobiohydrolase), N-acquiring enzymes (NAG, β-1,4-*N*-acetylglucosaminidase, LAP; leucine aminopeptidase), and oxidase (PERX; peroxidase, PO; phenol oxidase) (Saiya-Cork et al., 2002). One gram of fresh soil was weighed and then dispensed in 50 mL of buffer. The sample well, quenching well, reference standard well, blank well, and negative control well were established in the plate. The standard substance 4-methylumbelliferone (4-MUB) was used for CBH, BG and NAG, and the standard substance 7-amino-4-methylcoumarin (AMC) was applied only to LAP. The enzyme substrate (L-DOPA) was used for oxidase. Our previous study described in detail the amount added to each well, the incubation time of the experiment, and measurement setting parameters (Su et al., 2023).

The soil exocellular enzyme activity coefficient was calculated as follows:

$$\text{Exocellular enzyme activity coefficient} = \frac{\text{Carbon (nitrogen) enzyme activities}}{\text{MBC (MBN)}} \quad (1)$$

### 2.4. Determination of soil amino sugar

The content of soil amino sugars was measured by hydrolysis, purification and derivatization according to Zhang and Amelung (1996). In short, approximately 0.5 g air-dried soil (<0.25 mm) was weighed and hydrolyzed at 105 °C for 8 h in an autoclave using 6 M HCl (105 °C, 8 h). Afterward, the sample was purified by the standard procedure of centrifugation, freeze-drying and blowing nitrogen gas. Later, derivatization reagents were prepared to derivatize the dried sample, which was dissolved by adding 1.5 mL dichloromethane. Subsequently, the derivatives were dissolved in a mixture of ethyl acetate and hexane (v/v = 1:1) and detected with an Agilent 6890A gas chromatograph. Myo-inositol, as an internal standard, was used for the quantification of amino sugars before hydrolysation.

The total contents of amino sugar (TAS) were equal to the sum of muramic acid (MurN), galactosamine (GalN), and glucosamine (GluN). Fungal-GluN (F-GluN) was used as an indicator of soil fungal residues. As GluN was found in both cell walls of bacteria and fungi, F-GluN was calculated based on a molar ratio of MurN to GluN of 1:2 in bacterial cells (Li et al., 2015). Therefore, F-GluN was calculated as follows:

$$\text{F} - \text{GluN} = \text{GluN} - 2 \times \text{MurN} \times 179/251.2 \quad (2)$$

where the GluN molecular weight is 179, and the MurN molecular weight is 251.2.

The fungal-GluN/bacterial MurN ratio represents the relative contribution of fungi to bacterial residues. Fungal necromass C (FNC) was equal to multiplying the F-GluN content by 9, and bacterial necromass C (BNC) was equal to multiplying the bacterial-MurN content by 45, where 9 and 45 are the conversion coefficients of fungal GluN to FNC and bacterial MurN to BNC, respectively (Liang et al., 2019). The MNC was calculated as FNC plus BNC. The MNC in SOC represents the contribution of microbial necromass carbon to SOC. In addition, we calculated the necromass accumulation coefficient (NAC) (Wang et al., 2022a) as follows:

$$\text{NAC} = \frac{C_{Necromass}}{C_{living\ biomass}} \quad (3)$$

### 2.5. Soil lignin phenol determination

According to Feng and Simpson (2007), alkaline cupric oxide (CuO) was used to measure lignin phenol. In brief, 1–2 g soil samples (<0.15 mm), 100 mg of ammonium iron sulfate hexahydrate ($Fe(NH_4)_2(SO_4)_2{\cdot}6H_2O$) and 1 g of CuO were weighed and added to a Teflon tube and then heated (170 °C, 2 h) combined with a 2 M sodium hydroxide (NaOH) solution. After cooling, ethyl vanillin, as a recovery standard, was added to the oxidation products of lignin. Afterward, 6 M HCl was used for further acidification. Ethyl acetate was used repeatedly to extract the supernatant after centrifugation, and trans-cinnamic acid was then added as a quantified internal standard and finally dried using nitrogen gas. The lignin oxidation products were then derivatized prior to quantification. An Agilent gas chromatograph instrument was employed to quantify the lignin phenol.

The total lignin phenols (TLP) can be expressed as three types of phenols, including vanillyl types (V: acetovanillone + vanillic acid + vanillin), syringyl types (S: syringic acid + acetosyringone + syringaldehyde), and cinnamyl types (C: *p*-coumaric acid + ferulic acid). The TLP is equal to the sum of the three types of phenols. In addition, we calculated the ratios of acid/aldehyde for V phenol ((Ad/Al)v) and S phenol ($(Ad/Al)_s$) and the ratios of C/V and S/V phenols to indicate the

degradation of lignin (Chen et al., 2021). The calculation of the TLP in SOC reflected the contribution of lignin phenols to SOC.

### 2.6. SOC fraction

SOC fractions were separated by the particle-size method (Gill et al., 1999). Soil samples (10 g) were weighed into white bottles, and 50 mL of 5 g/L (w/v) sodium hexametaphosphate ($(NaPO_3)_6$) solution was added and shaken at 90 r $min^{-1}$ for 18 h in a shaker. Sizes of different sizes (250 μm and 53 μm) were used to collect different fractions. The fraction remaining on the 250 μm sieve was collected as cPOC (>250 μm), the fraction passing through 250 μm but remaining on the 53 μm sieve was collected as fPOC (53 μm–250 μm), and the fraction passing through the 53 μm sieve was collected as MAOC (<53 μm). In the process of particle size classification, we rinsed the soil with deionized water until the water was no longer muddy. Each SOC fraction (cPOC, fPOC and MAOC) was dried and weighed at 60 °C for the determination of SOC content, which was assayed via the dichromate oxidation method. The results of mass recovery are listed in Table S3.

### 2.7. Solid-state $^{13}C$ NMR spectroscopy analysis

NMR spectroscopy was employed to analyze the SOC chemical composition. In brief, approximately 8 g of soil was weighed, and 10 % HF solution (50 mL) was added to centrifugation tubes. The mixture was shaken in a shaker (1 h) and then centrifuged at 3000 rpm for 10 min. After removing the clear supernatant, the residues were treated with HF eight times. The times for reacting were 1 h (the times of first to fourth), 12 h (the times of fifth to seventh times) and 24 h (the last time). To remove the remaining HF solution, deionized water was used to rinse the sediment. Later, an oven was used to dry the sediment at 40 °C, followed by sieving at 0.25 mm for analysis. The NMR spectrometer was an AVANCE III HD 600 MHz from Bruker BioSpin equipped with a H/X double resonance solid probe (Man et al., 2021). The $^{13}C$ NMR spectrum is mainly classified into four functional regions, including alkyl C (0–45 ppm), O-alkyl C (45–110 ppm), aromatic C (110–160 ppm), and carbonyl C (160–220 ppm). The $^{13}C$ NMR spectra of each sample can be seen in the supplementary information (Spectra Figures).

### 2.8. Data analysis

The data normality was tested using the Shapiro–Wilk statistic, and the homogeneity of variance was analyzed by the Levene statistic. One-way analysis of variance (ANOVA) was used to compare the significant differences in soil basic properties, enzyme activities, PLFAs, TLP, MNC, SOC physical fractions and chemical structures during vegetation restoration. Statistically significant differences were evaluated at the 0.05 level ($P < 0.05$). Duncan's test was performed to conduct multiple comparisons at statistical significance. Regression analyses were used to explore the relationship between lignin phenols, microbial necromass and other environmental variables. Pearson's correlation analysis was used to examine the relationships between lignin phenols, microbial necromass, SOC physical fractions, SOC chemical structure and environmental factors. In addition, the effects of controlling variables on the lignin phenols and microbial necromass were studied using partial least squares path modeling (PLS-PM). Statistical analyses were conducted using IBM SPSS statistics 20. The "PLS-PM" package was used for the analysis in R 3.6.2. Graphs were plotted by Origin (version 2017).

## 3. Results

### 3.1. Vegetation and soil properties

Compared with farmland, vegetation restoration increased the concentrations of SOC, TN, DOC, DON, EOC, MBC, MBN and SWC (Table S4, $P < 0.05$). The AGB also gradually increased from 15Y—45Y. Conversely, soil TP, SAP, pH, and BD gradually decreased with vegetation restoration. However, there was no significant influence of vegetation restoration on soil silt and sand (Table S4, $P > 0.05$).

### 3.2. Soil enzyme activities and microbial PLFAs

The hydrolase activities of CBH, BG, and NAG increased significantly along the age gradient, while the activities of PERX, PO and LAP decreased following the vegetation restoration stages (Fig. 2). There was no significant difference in C-acquiring enzyme/MBC during vegetation restoration (Fig. 2g), while the N-acquiring enzyme/MBN decreased significantly with stand age (Fig. 2h). Restoration age had minor effects on the total PLFAs, bacteria (GP and GN bacteria), fungi and actinomycete PLFAs (Fig. S1, $P > 0.05$).

### 3.3. Soil lignin phenol contents

Compared with farmland, vegetation restoration had no significant effects on the contents of TLP, V and S phenols (Fig. 3a, $P > 0.05$) but reduced C-type phenols in *R. pseudoacacia* soil ($P < 0.05$; Fig. 3a). The TLP in SOC changed from 5.03 to 20.08 g $kg^{-1}$ SOC. In comparison to farmland, plantations aged 15–45Y years showed 35–46 % decreases in the proportion of TLP in SOC (Fig. 3b, $P < 0.05$). However, the TLP in SOC showed a negligible difference among the 15–45Y soils. Compared to the farmland, the 15–45Y soils reduced the proportions of S-type and C-type phenols in SOC (Fig. 3b) but had no significant effect on the proportion of V-type phenols in SOC ($P > 0.05$). There were 1.3–1.4 times and 1.3–1.9 times greater ratios of S/V and C/V in the control compared with 15–45Y soils ($P < 0.05$; Fig. 3c–d), while the $(Ad/Al)_V$ ratio and $(Ad/Al)_S$ ratio increased with vegetation restoration ($P < 0.05$; Fig. 3e–f).

### 3.4. Soil amino sugar contents and microbial necromass

The TAS contents progressively increased with vegetation restoration and attained their maximum at 35Y (Table S5). MurN, GluN and GalN also maintained a similar trend ($P < 0.001$; Table S5). Compared to farmland, vegetation restoration increased the FNC by 1.4–2.4 times and the BNC by 1.8–2.5 times at 35Y and 45Y, resulting in increases by 1.5–2.4 times in the MNC ($P < 0.01$; Fig. 4a). At 35Y and 45Y, vegetation restoration improved FNC contributions to SOC by 0.7–1.4 times and increased BNC contributions to SOC by 1.0–1.4 times, respectively, resulting in 0.8–1.4 times greater MNC contributions to SOC than that observed in farmland (Fig. 4b).

### 3.5. SOC physical fractions and chemical composition

Vegetation restoration significantly increased the organic C contents in cPOC, fPOC, POC, and MAOC ($P < 0.01$, Fig. 5a–d). POC/SOC progressively increased along with revegetation, while MAOC/SOC gradually declined when compared with farmland ($P < 0.05$, Fig. 5g–h). Moreover, the main functional group of O-alkyl C had the highest intensity at 44–48 % (Fig. 6). Vegetation restoration enhanced the O-alkyl C intensity by 1.3 %–3.5 % compared to farmland ($P < 0.05$, Fig. 6). Nevertheless, there were negligible changes in the other three functional groups during vegetation restoration ($P > 0.05$).

### 3.6. Controls on soil lignin phenols and microbial necromass

Regression analyses revealed that NAG and SWC were significantly negatively correlated with TPL in SOC (Fig. 7). In addition, MNC in SOC was significantly positively correlated with soil properties (SWC, TN, clay) but negatively associated with soil pH and LAP enzyme activities (Fig. 7). A significant positive relationship was found between soil carbon fractions and vegetation and soil properties (AGB, SOC, TN, DOC, DON, and MBC), but a significant negative correlation was found with

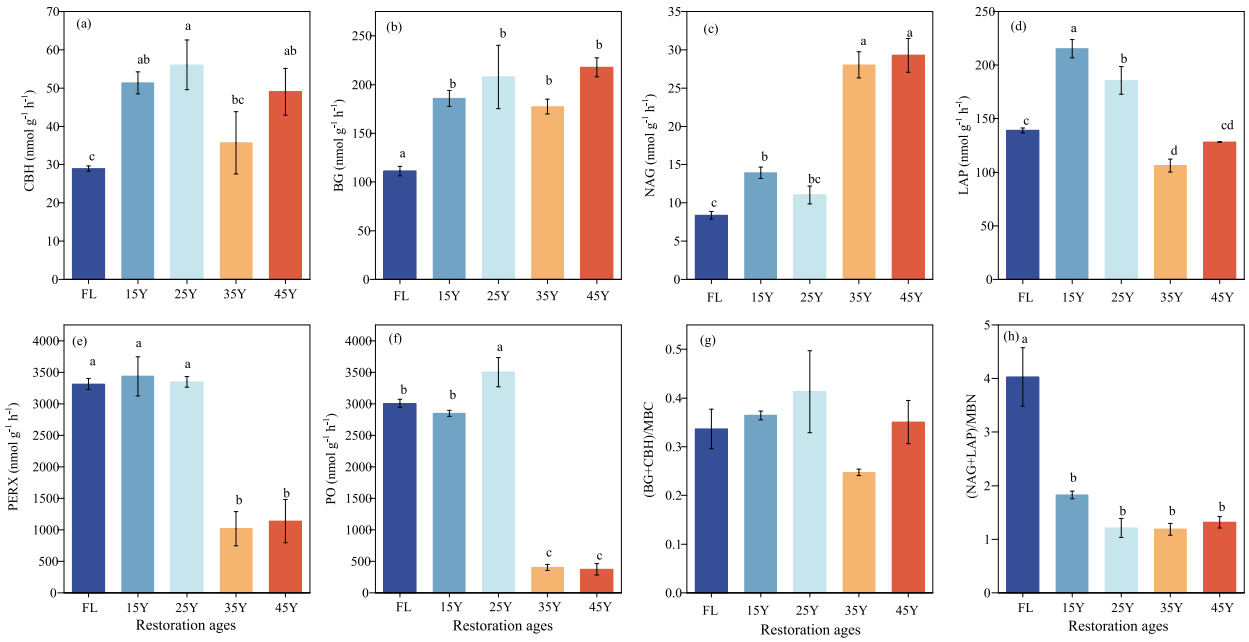


**Fig. 2.** Effects of vegetation restoration ages on the potential activity of soil extracellular enzymes: (a) CBH, cellobiohydrolase; (b) BG, β-1,4-glucosidase; (c) NAG, β-1,4-*N*-acetylglucosaminidase; (d) leucine aminopeptidase (LAP); (e) PERX, peroxidase; (f) PO, phenol oxidase. (g)–(h) represent the C-acquiring and N-acquiring enzyme coefficients. Error bars represent standard errors of the means (n = 3). Different letters indicate significant differences among treatments at $P < 0.05$.

soil oxidase enzyme activities (Fig. S2).

PLS-PM was used to disentangle the direct and indirect relationships between two biomarkers and other environmental factors, and the explanation rates of variance were 70 % and 84 %, respectively (Fig. 8). Restoration age indirectly decreased the TLP contribution to SOC by influencing AGB (standardized total effect = −0.63) and (Ad/Al)v (standardized total effect = −0.43). Furthermore, vegetation restoration increased AGB (standardized total effect = −0.44) and decreased LAP activity (standardized total effect = −0.71), which promoted soil TAS preservation and indirectly increased the contribution of MNC to SOC.

## 4. Discussion

Vegetation restoration increased the SOC content, but the contributions of TLP to SOC and MNC to SOC showed different trends. Specifically, when compared to farmland, vegetation restoration decreased the contribution of TLP to SOC, whereas there was a negligible difference in the contribution among different stand ages. Plant carbon input and plant-derived carbon degradation may jointly regulate the accumulation of lignin phenols. In addition, vegetation restoration promoted MNC accumulation and the contribution of MNC to SOC in the late stage, which may be attributable to the combined effects of increased residue preservation and decreased LAP enzyme activity, which inhibited the mineralization decomposition of microbial necromass. Moreover, vegetation restoration altered the SOC physical fractions and chemical composition. The increase in the overall carbon pool, including an increase in the MAOM pool, suggests a positive impact on carbon stability.

### *4.1. Vegetation restoration promoted SOC formation by adjusting plant-derived carbon and microbial-derived carbon*

Afforestation markedly promoted SOC formation in the topsoil (0–20 cm), which is favoured by the sequestration of SOC. Soil organic carbon is a continuum of constantly decomposing organic compounds, with the decomposition of plant residues accompanied by the formation of microbial residues. Hence, plant-derived carbon and microbial-derived carbon are two principal SOC sources (Kögel-Knabner, 2002). In our study, we found divergent accumulation patterns of plant-derived carbon and microbial-derived carbon during afforestation.

In terms of plant-derived carbon, our study revealed that vegetation restoration had a negligible influence on the TLP content (Fig. 3a) but had a significant effect on SOC-normalized lignin phenols (Fig. 3b). SOC-normalized lignin phenols were higher in farmland soil than in *R. pseudoacacia* plantation soil (Fig. 3b), which shows a similar result to Liu et al. (2022b), who found that natural restoration reduced TLP in SOC compared with farmland. This may be because when compared with forest ecosystems, farmland soil habitats are unsuitable for lignin decomposers, such as white-rot fungi (Thevenot et al., 2010). However, there was no considerable difference in TPL in SOC among 15–45Y stand ages. The balance between the input and output of plant-derived C may jointly regulate plant-derived lignin accumulation (Wang et al., 2022b). Aboveground biomass increased, but the total lignin phenol content did not increase with stand age. The absence of lignin accumulation is mainly ascribed to the enhancement of lignin oxidase decomposition (Li et al., 2020). One study reported that higher (Ad/Al)v and (Ad/Al)s represented an increase in microbial oxidation for side chains (Yang et al., 2022b), and decreasing S/V and C/V indicated more advanced microbial transformation stages (Chen et al., 2021). Our results showed that S/V and C/V decreased; conversely, (Ad/Al)v and (Ad/Al)s increased with stand age (Fig. 3c–f), which supported the gradual increase in the microbial oxidation and decomposition ability of lignin from 15Y to 45Y. Therefore, stand age did not alter lignin phenol in SOC in large part because of the interaction of plant C degradation and input. Jia et al. (2021) also showed that stand age affected aboveground biomass but did not significantly influence lignin phenol accumulation. They concluded that plant diversity but not stand age was an important driver of lignin accumulation.

A growing number of studies have demonstrated that MNCs are a key pathway for SOC formation (Shao et al., 2019; Wang et al., 2021b). Compared with plant-derived components, vegetation restoration promoted the accrual of MNC and its contribution to SOC (Fig. 4). This result is in agreement with our second hypothesis and is similar to the reforestation result of Shao et al. (2019). This may be ascribed to two reasons. First, plant carbon input provided substrate for microbial growth, which is favorable to microbial proliferation and produces more residue materials (Li et al., 2020; He et al., 2021), as revealed by the

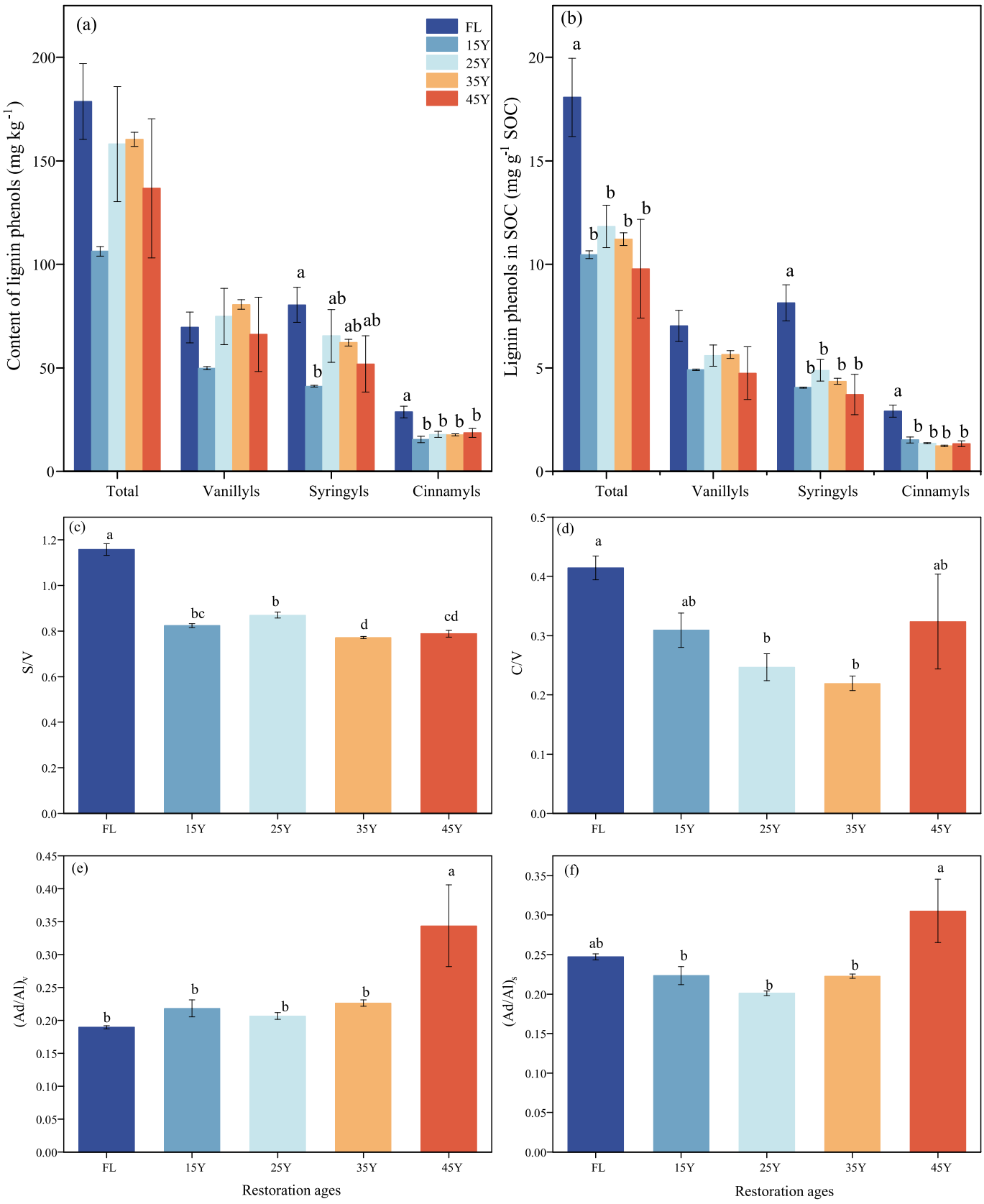


**Fig. 3.** Effects of vegetation restoration ages on (a) total and individual lignin phenol contents in soil; (b) proportion of lignin phenols in soil organic carbon; (c) ratio of syringyl-type to vanillyl-type monomer (S/V); (d) ratio of cinnamyl-type to vanillyl-type monomer (C/V); (e) acid-to-aldehyde ratio of vanillyl-type lignin monomer (Ad/Al)V; (f) acid-to-aldehyde ratio of syringyl-type monomer (Ad/Al)s. Error bars represent standard errors of the means (n = 3). Different letters indicate significant differences among treatments at $P < 0.05$.

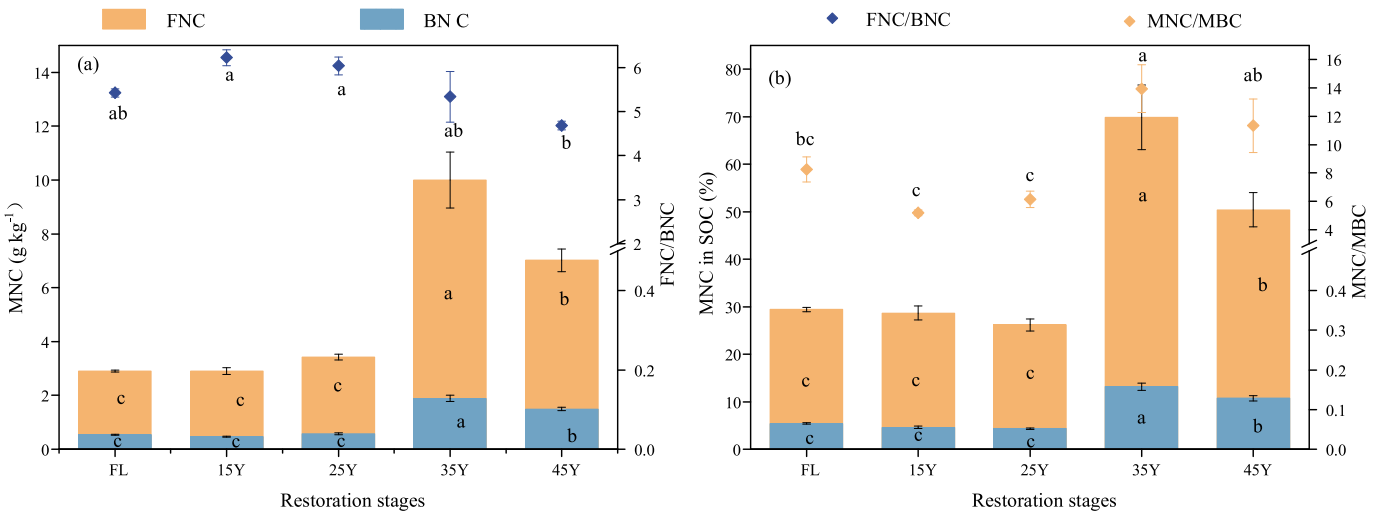


**Fig. 4.** Effects of vegetation restoration ages on (a) microbial necromass C and ratio of fungal to bacterial necromass C in soil and (b) the proportion of microbial necromass C in SOC and the necromass accumulation coefficient (MNC/MBC). Error bars represent standard errors of the means (n = 3). Different lowercase letters indicate significant differences in fungal and bacterial necromass C and total microbial necromass C among treatments at $P < 0.05$, respectively. MNC: microbial necromass carbon; FNC/BNC: fungal necromass carbon/bacterial necromass carbon; MNC in SOC: microbial necromass carbon in soil organic carbon; MNC/MBC represents the necromass accumulation coefficient.

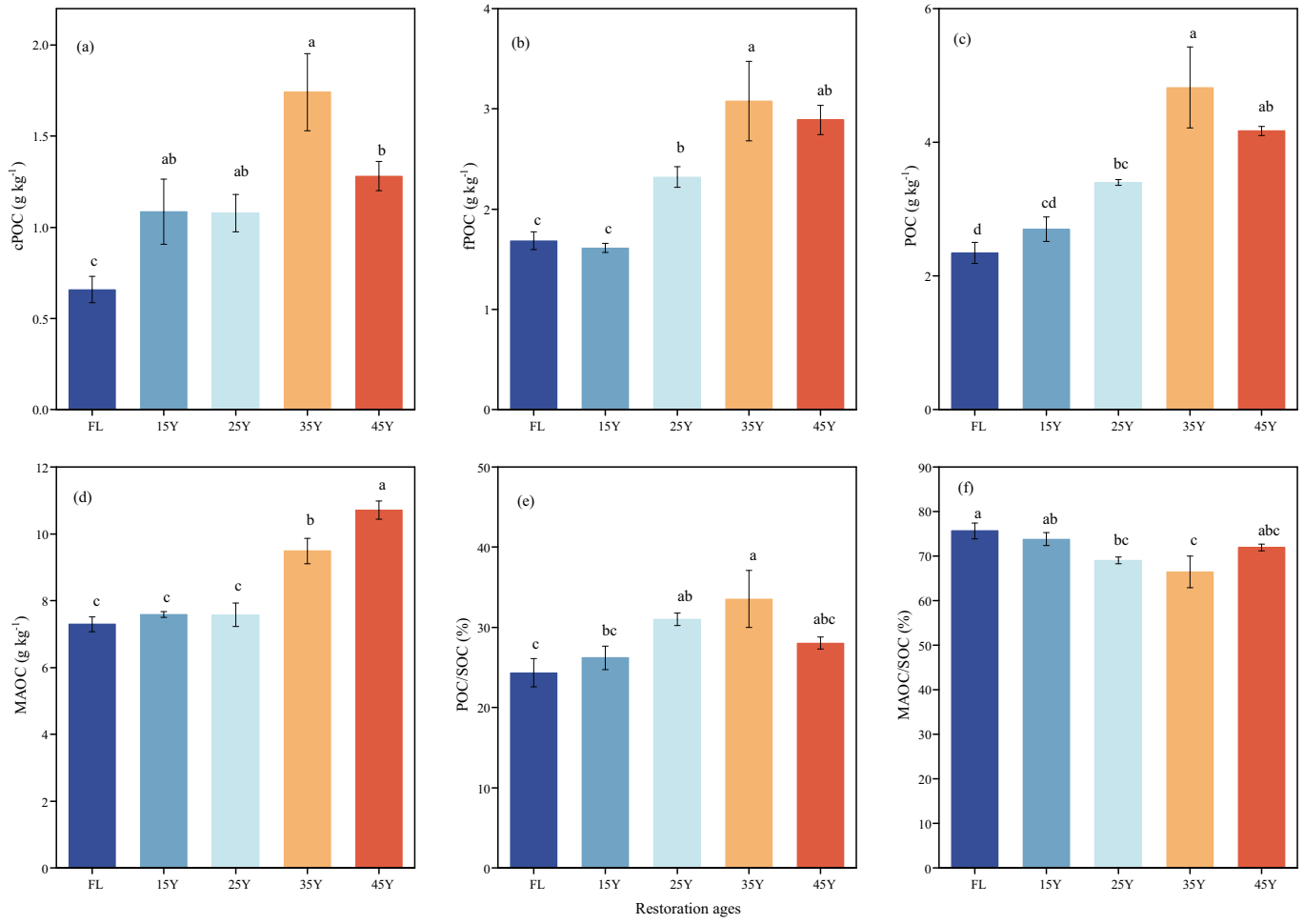


**Fig. 5.** Effects of vegetation restoration ages on physical fractions of soil organic carbon (SOC). cPOC, coarse particulate organic carbon; fPOC, fine particulate organic carbon; MAOC, mineral-associated organic carbon; POC, particulate organic carbon; MAOC/SOC, mineral-associated organic carbon/soil organic carbon; POC/SOC, particulate organic carbon/soil organic carbon. Error bars represent standard errors of the means (n = 3). Different letters indicate significant differences among treatments at $P < 0.05$.

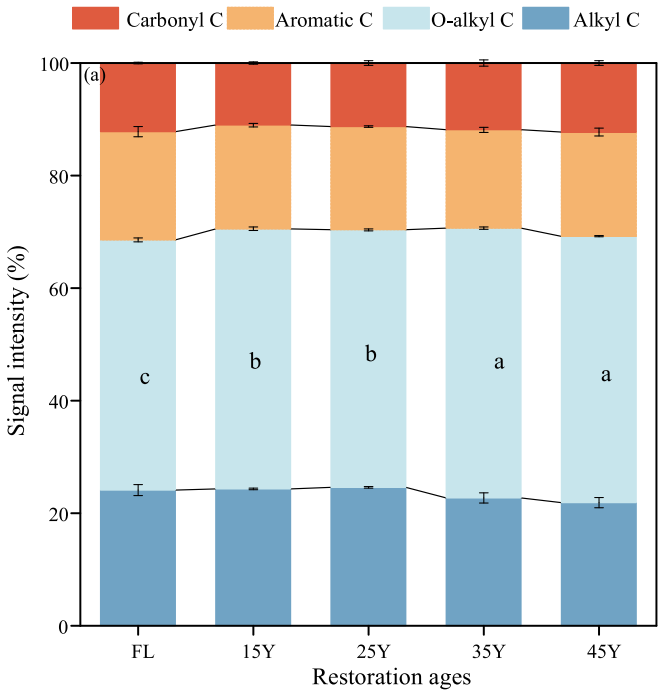


**Fig. 6.** Effect of vegetation restoration ages on the relative intensity distribution of the chemical shift in $^{13}C$ NMR spectra in soil. Error bars represent standard errors of the means (n = 3). Different letters indicate significant differences among treatments at $P < 0.05$.

increase in MBC and MNC (Table S4, Fig. 4). Second, compared with recalcitrant plant-derived C, microbial necromass is considered an N-rich organic substrate (Liang et al., 2019). Microbial necromass can be reutilized by microorganisms by secreting N-acquiring enzymes (Cui et al., 2020). Sufficient nutrients accelerate soil microbial necromass accrual in soil, while the absence of nutrients limits microbial necromass retention (Shao et al., 2021). Soil nitrogen availability increased from farmland to plantations (Table S4), hence inhibiting the enzyme activity of LAP and the nitrogen-acquiring enzyme coefficient (Fig. 2d, h), which implied that microbial demand for nitrogen acquisition decreased. Thus, this further suppressed necromass decomposition and favoured the accrual of microbial residues. This result was supported by LAP enzyme activities being negatively associated with the MNC in SOC (Fig. 7), which indicated that vegetation restoration is beneficial to the preservation of microbial necromass in SOC by inhibiting N-acquiring enzyme activities. Moreover, a higher necromass accumulation coefficient was observed in the 35–45Y soils, which represented more efficient preservation of microbial necromass (Wang et al., 2022a). Thus, vegetation restoration leads to an increase in microbial necromass input by increasing plant input and the necromass accumulation coefficient and to a reduction in residue decomposition by decreasing LAP enzyme activities, which is beneficial to necromass preservation.

In addition, FNC was more advantageous than BNC in the SOC formation process during vegetation restoration (Fig. 4), indicating that fungal necromass is given priority in soil preservation. This may be attributed to several reasons. First, the fungal cell wall is more recalcitrant and more difficult to break down than the bacterial cell wall (Li et al., 2015; Zhao et al., 2022). Second, there is a higher range of ratios of biomass carbon to nitrogen and carbon use efficiency of fungi than that of bacteria, which results in higher fungal biomass and necromass carbon production (Luo et al., 2022). Third, fungal necromass is more stabilized in the soil by interactions between fungal residues and tannins (Adamczyk et al., 2019).

### 4.2. Vegetation restoration altered SOC pools and their stability

Afforestation profoundly altered the accumulation of SOC fraction in the top layer (0–20 cm). Vegetation restoration enhanced the POC pool (Fig. 5). Dong et al. (2022) also claimed that plantations increased the content or stocks of POC compared with farmland. POC mainly consists of relatively undegraded plant detritus and is less protected, and land use changes may alter the decomposition rate of POC (Lavallee et al., 2019). Hence, the enhancement of the POC pool can be attributed to gradually increasing plant input and decreasing microbial decomposition. Vegetation restoration induced an increase in AGB, which is a major source of SOC (Dong et al., 2022). There was a positive correlation between AGB and POC (Fig. S2), indicating that the enhancement of POC was partially due to the input of plant detritus. Furthermore, POC was negatively correlated with oxidase enzymes (Fig. S2), and the decrease in oxidase enzymes may lead to the slower decomposition of POC with vegetation restoration. In terms of chemical constituents, POC includes many plant-derived components, such as phenols, celluloses, hemicelluloses, and plant-derived lipids (Lavallee et al., 2019; Angst et al., 2021). We observed that the content of POC increased but the total lignin phenols decreased during vegetation restoration, suggesting that other plant-derived components (i.e., lipids) may contribute to the accumulation of POC (Dai et al., 2022).

Compared with farmland, vegetation restoration increased the MAOC pool. Dong et al. (2022) and Yang et al. (2023) also claimed that forestland has a higher MAOC content than farmland in the top layer of 0–20 cm soil. The response of increased MAOC to vegetation restoration could be explained by two reasons. First, microbial necromass, as a primary source of stable SOC, promotes the formation of MAOC by physically or chemically absorbing mineral particles, which plays a crucial part in long-lasting SOC accrual (Liang et al., 2019; Liao et al., 2022). The MAOC pool represents the relatively stable organic carbon repository, which can associate with minerals to protect from decomposition; therefore, it has a longer mean residence time than POC (Lavallee et al., 2019; Yang et al., 2023). We observed that vegetation restoration increased the MNC content (Fig. 4), which likely promoted the formation of MAOC via interactions of microbial necromass with the mineral surface. Second, the pathway of direct sorption also contributes to the formation of MAOC (Sokol et al., 2018), and dissolved organic carbon (DOC) serves as a vital carbon source for mineral carbon stocks in high-leaching forest soil (Sokol et al., 2018). Afforestation increased the content of soil dissolved organic carbon in our study (Table S4), likely promoting the direct sorption of low molecular dissolved organic matter on the surface of mineral particles and thus the contribution of the direct sorption pathway to MAOC formation. Consequently, the two pathways of direct sorption of carbon substrate and microbial transformation may make a joint contribution to MAOC accumulation. The afforestation process increased the concentration of the MAOC fraction, implying enhanced carbon persistence. The increase in the overall carbon pool during vegetation restoration, including an increase in the stable MAOC pool, suggests a positive impact on carbon stability and thus on long-term soil C sequestration.

Vegetation restoration also altered the distribution proportion of carbon fractions in SOC and the chemical structure. We found that revegetation significantly improved the proportion of POC/SOC (Fig. 5e) but decreased the proportion of MAOC/SOC (Fig. 5f). These results likely reflect a rapid increase in the nonprotected organic carbon pool owing to the relatively rich source of SOM following vegetation restoration (Li et al., 2022a). Based on $^{13}C$ NMR analysis, O-alkyl C is a major form of SOC, which has also reported in other forest soils (Yang et al., 2022a). Vegetation restoration significantly enhanced the proportion of O-alkyl C (Fig. 6). O-alkyl C largely originates from cellulose, hemicellulose, and other polymerized and nonpolymerized carbohydrates (Lan et al., 2022), which can be easily decomposed or mineralized if in contact with specific decomposers (Mustafa et al., 2022). The potential reason for the increase in O-alkyl C is mainly the higher POM

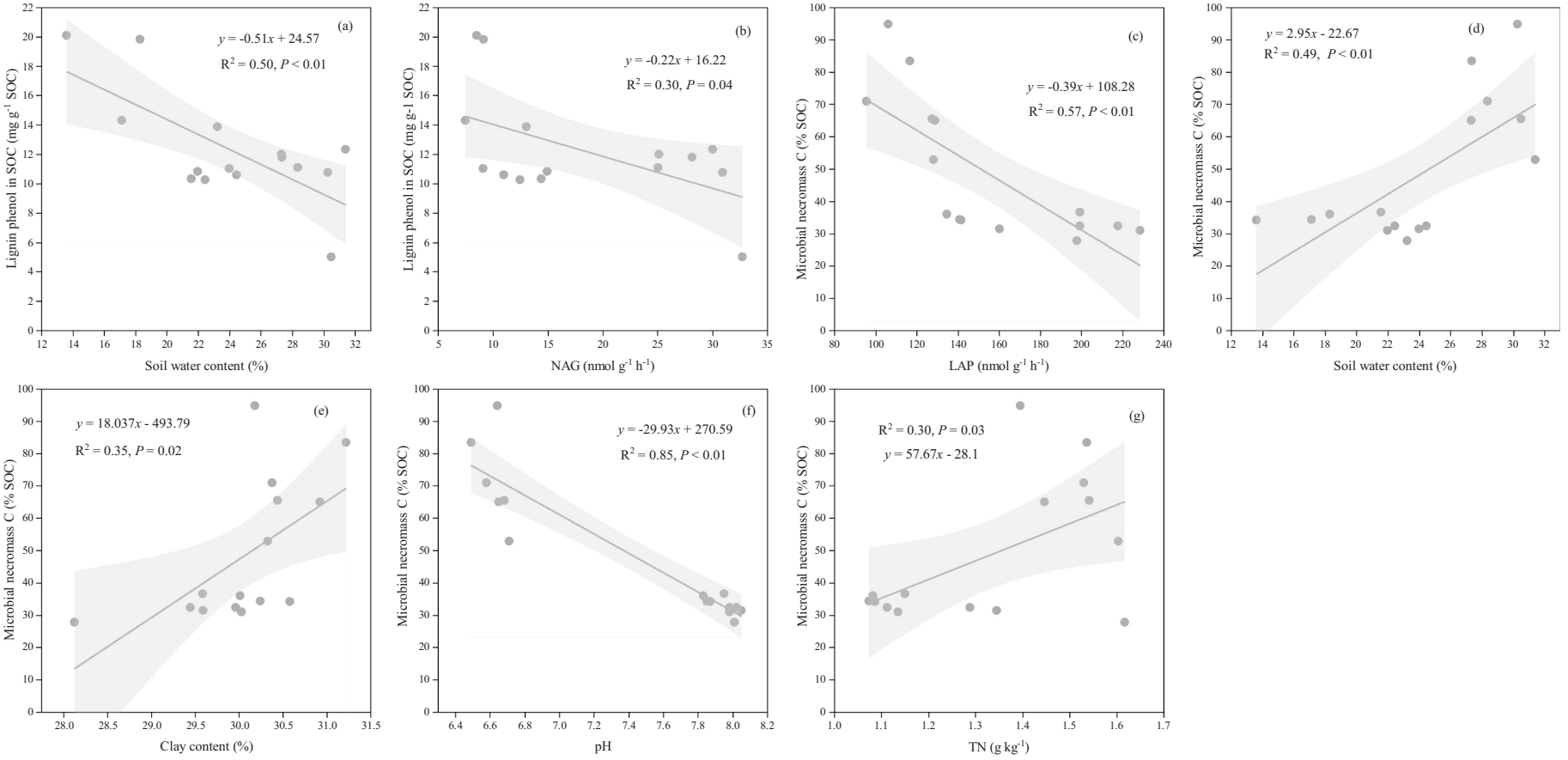


**Fig. 7.** Regression analysis between lignin phenols in SOC and microbial necromass C (% SOC) with soil enzyme activities and soil properties. (a–b) The relationship of lignin phenols in SOC with soil water content and NAG enzyme activities. (c–g) are the relationships of microbial necromass C (% SOC) with LAP enzyme activities, soil water content, clay content, pH and soil total nitrogen content, respectively.

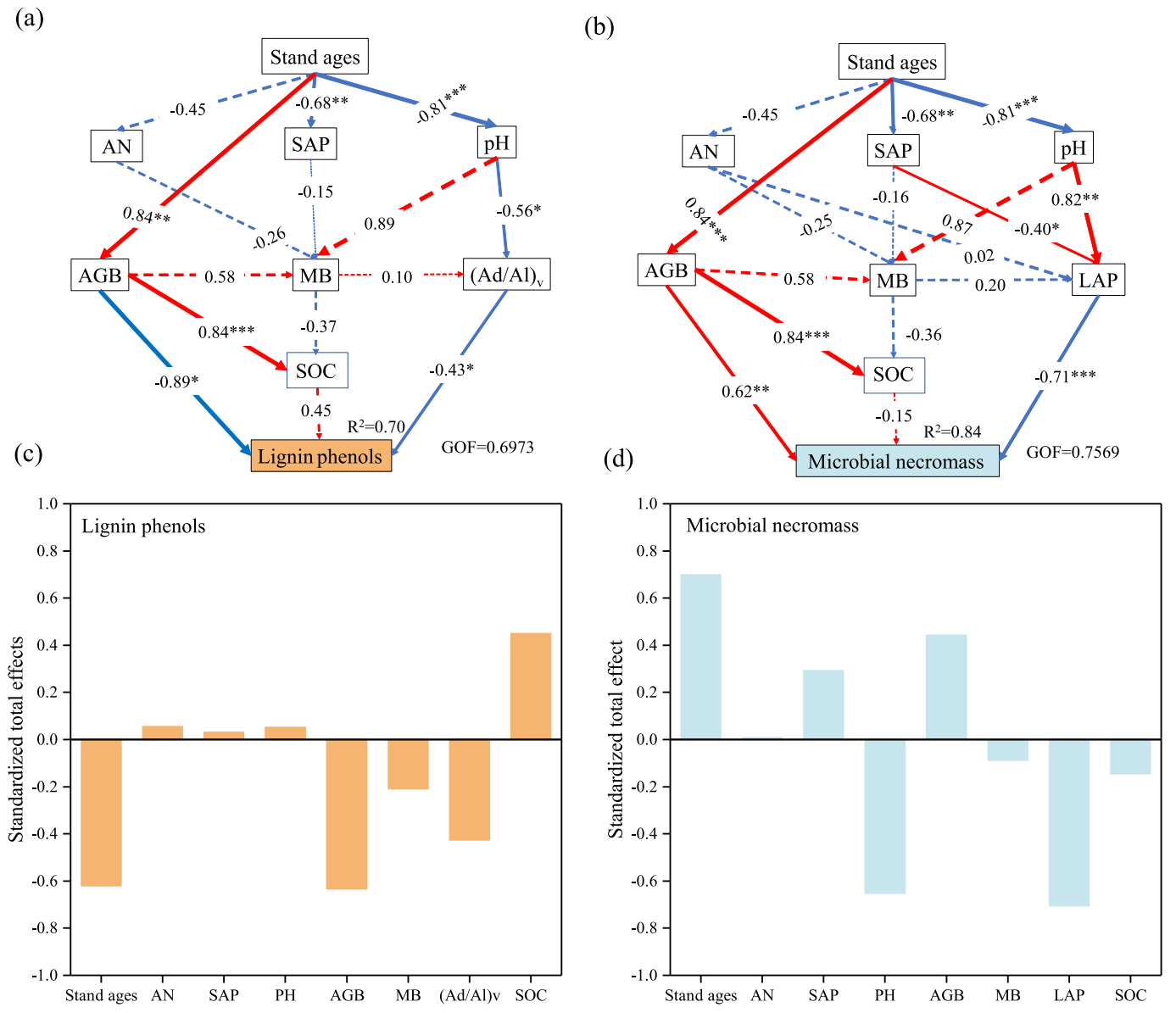


**Fig. 8.** Partial least squares path modeling (PLS-PM) showing the effects of vegetation restoration ages on lignin phenols (a) and microbial necromass (b) and standardized total effects of environmental variables derived from the PLS-PM (c, d). Red arrows represent positive relationships, and blue arrows represent negative relationships. The solid arrows represent significant relationships (*$P < 0.05$, **$P < 0.01$, ***$P < 0.001$), and the dashed arrows represent nonsignificant relationships. The width of the arrow represents the size of the path coefficient. $R^2$ values indicate the variance of variables accounted for by the model. GOF, goodness of fit; AN, ammonia nitrogen; SAP, soil available phosphorus; PH, soil pH values; AGB, aboveground biomass; MB: fungal and bacterial phospholipid fatty acids; Oxidase, phenol oxidase and peroxidase, SOC, soil organic carbon; LAP, leucine aminopeptidase; Lignin phenol, SOC-normalized lignin phenol; Microbial necromass, SOC-normalized microbial necromass.

proportion driven by the afforestation process (Fig. S2). In contrast, vegetation restoration did not change the alkyl C intensity. The alkyl C group originates from original plant biopolymers and the metabolic products of soil microorganisms and is considered stable C (Lan et al., 2022). Hence, vegetation restoration altered the SOC physical fraction and chemical composition.

### 4.3. Factors influencing SOC formation and accumulation

The accumulation of lignin phenol is influenced by various factors. Water availability is a major control factor for plant decomposition (Zhong et al., 2017). Microbial growth and activities decrease under arid conditions, which limits plant carbon decomposition (Ma et al., 2018). In this study, a significant positive correlation existed between SWC and (Ad/Al)v, but a negative correlation was found between SWC and lignin phenol in SOC (Fig. S2), indicating that an increase in the soil water content favoured lignin decomposition but favoured lignin phenol preservation less. In addition, lignin decomposition is influenced by soil enzyme activities (Wang et al., 2020). NAG enzyme activity was positively correlated with (Ad/Al)v (Fig. S2) but negatively correlated with SOC-normalized lignin in our findings (Fig. 7), which revealed that NAG decreased the contribution of TLP to SOC by promoting lignin decomposition. In addition to exocellular enzyme activities, the microbial community structure regulates lignin decomposition; for example, fungi are a major participant in lignin decomposition (Thevenot et al., 2010; Li et al., 2020; Luo et al., 2022; Wang et al., 2022b). Nonetheless, based on the PLFA results, we did not observe obvious correlations between fungi and lignin phenols. Hence, future research should emphasize the function of microbial degradation and gene abundance in recalcitrant and complex substances to further explore the microbial mechanism of

lignin decomposition.

Microbial necromass accumulation can be mediated by biotic and abiotic factors. He et al. (2021) reported that the preservation of microbial residues can be regulated by soil moisture. Our results found that the MNC in SOC increased with increasing water availability (Fig. 7). Soil moisture regulates microbial residues in two ways. First, the increase in soil water availability not only directly promotes microbial activities but also improves microbial substrate availability, accelerating necromass formation and accrual (Mou et al., 2021). Moreover, the increase in soil moisture leads to more plant carbon in the soil, which is conducive to transforming more active carbon via microbial biomass into microbial necromass (He et al., 2021). The accumulation of residues is closely associated with soil texture. The MNC in SOC significantly increased with the clay content (Fig. 7), which is consistent with the finding reported by Li et al. (2022c). Soil clay particles influence microbial necromass accumulation by promoting microaggregate formation or chemical bonds with mineral soils, which further suppresses necromass decomposition and utilization (Six et al., 2006; Chen et al., 2020). Soil pH values also exert a key influence in controlling microbial necromass accumulation. In our research, MNC in SOC increased with decreasing soil pH value, which is similar to the reports of Wang et al. (2021a) and Yang et al. (2022b). The following three reasons may be used for explanation. First, low pH may result in higher fungal growth and thus higher fungal necromass accumulation (Silva-Sánchez et al., 2019). Second, the lower soil pH is conducive to increasing microbial carbon use efficiency and microbial residue production (Yang et al., 2022b). Third, clay surfaces can closely bind with protonated carboxylic acid functional groups at lower pH values, which can strengthen the stabilization of microbial necromass (Newcomb et al., 2017). Furthermore, soil nitrogen affects microbial necromass accumulation. Soil total nitrogen was positively correlated with MNC in SOC in our study (Fig. 7). Generally, microbial necromass has a comparatively lower C/N. When the soil nitrogen is deficient, microbial necromass can be reused by microorganisms by mining nitrogen strategies; thus, soil has a lower conservation of microbial necromass. However, microorganisms decrease microbial residue reutilization in N-rich soil, accelerating the preservation of microbial necromass (Cui et al., 2020; Shao et al., 2021). As a result, these results confirm that basic soil properties (soil water content, clay, pH, and TN content) play an important role in regulating microbial necromass accrual.

### *4.4. Implications of afforestation on SOC sequestration*

Our results highlight that the afforestation process changed the SOC accumulation and molecular composition and increased the physical stability of the SOC pool. Compared with farmland, older stand ages are more beneficial for the accumulation of MNC, stable MAOC and SOC, which play an important role in SOC sequestration in the long run. Therefore, afforestation is an effective measure to restore degraded ecosystems, and it provides a scientific basis for evaluating the potential of soil carbon sequestration in plantations and effectively implementing ecosystem carbon sink management.

## 5. Conclusion

Clarifying the SOC source and composition provides a well-rounded perspective of SOC formation and stabilization under afforestation. Vegetation restoration affects SOC composition by altering plant-derived carbon and microbial-derived carbon. SOC-normalized lignin phenols decreased from farmland to plantation, presumably due to farmland being less favorable to lignin decomposers. However, there was a negligible difference in SOC-normalized lignin phenol among different stand ages, which may be determined by the interaction of lignin derivation input and lignin degradation. Conversely, vegetation restoration increased the content of MNC and the contribution of MNC to SOC. This mainly resulted from the enhancement of the necromass accumulation coefficient, decrease in microbial necromass decomposition due to decreased LAP enzyme activity, and improvement in microbial necromass preservation due to regulation of soil physiochemical properties. Moreover, revegetation favors the accumulation of POC and MAOC, which has a positive impact on carbon stability. In short, our research revealed the variations in SOC composition and stability during vegetation restoration, offering a theoretical foundation for vegetation restoration and soil carbon pool management in fragile habitats.

## CRediT authorship contribution statement

**Zhuoxia Su:** Conceptualization, Formal analysis, Investigation, Visualization, Writing – original draft. **Yangquanwei Zhong:** Methodology. **Xiaoyue Zhu:** Investigation, Methodology. **Yang Wu:** Methodology. **Zhifeng Shen:** Methodology. **Zhouping Shangguan:** Conceptualization, Data curation, Funding acquisition, Supervision, Writing – review & editing.

## Declaration of competing interest

The authors declare that they have no competing interests.

## Data availability

Data will be made available on request.

## Acknowledgments

We would like to thank the editors and anonymous reviewers for their constructive comments and suggestions. Our work was sponsored by the Science and Technology Innovation Program of the Shaanxi Academy of Forestry (SXLK2022-02-03), National Natural Science Foundation of China (42077452), the Key R&D and Promotion Special Projects of Henan Province (232102320260).

## Appendix A. Supplementary data

Supplementary data to this article can be found online at https://doi.org/10.1016/j.scitotenv.2023.165665.

## References

Adamczyk, B., Sietiö, O.M., Biasi, C., Heinonsalo, J., 2019. Interaction between tannins and fungal necromass stabilizes fungal residues in boreal forest soils. New Phytol. 223 (1), 16–21. https://doi.org/10.1111/nph.15729.

Angst, G., Mueller, K.E., Nierop, K.G.J., Simpson, M.J., 2021. Plant- or microbial-derived? A review on the molecular composition of stabilized soil organic matter. Soil Biol. Biochem. 156, 108189 https://doi.org/10.1016/j.soilbio.2021.108189.

Blair, G.J., Lefroy, R.D., Lisle, L., 1995. Soil carbon fractions based on their degree of oxidation, and the development of a carbon management index for agricultural systems. Aust. J. Agric. Res. 46, 1459–1466. https://doi.org/10.1071/AR9951459.

Bradford, M.A., Wieder, W.R., Bonan, G.B., Fierer, N., Raymond, P.A., Crowther, T.W., 2016. Managing uncertainty in soil carbon feedbacks to climate change. Nat. Clim. Chang. 6, 751–758. https://doi.org/10.1038/nclimate3071.

Brookes, P., Landman, A., Pruden, G., Jenkinson, D., 1985. Chloroform fumigation and the release of soil nitrogen: a rapid direct extraction method to measure microbial biomass nitrogen in soil. Soil Biol. Biochem. 17, 837–842. https://doi.org/10.1016/0038-0717(85)90144-0.

Chen, G., Ma, S., Tian, D., Xiao, W., Jiang, L., Xing, A., Zou, A., Zhou, L., Shen, H., Zheng, C., Ji, C., He, H., Zhu, B., Liu, L., Fang, J., 2020. Patterns and determinants of soil microbial residues from tropical to boreal forests. Soil Biol. Biochem. 151, 108059 https://doi.org/10.1016/j.soilbio.2020.108059.

Chen, X., Hu, Y., Xia, Y., Zheng, S., Ma, C., Rui, Y., He, H., Huang, D., Zhang, Z., Ge, T., Wu, J., Guggenberger, G., Kuzyakov, Y., Su, Y., 2021. Contrasting pathways of carbon sequestration in paddy and upland soils. Glob. Chang. Biol. 27, 2478–2490. https://doi.org/10.1111/gcb.15595.

Cui, J., Zhu, Z., Xu, X., Liu, S., Jones, D.L., Kuzyakov, Y., Shibistova, O., Wu, J., Ge, T., 2020. Carbon and nitrogen recycling from microbial necromass to cope with C:N stoichiometric imbalance by priming. Soil Biol. Biochem. 142, 107720 https://doi.org/10.1016/j.soilbio.2020.107720.

Dai, G., Zhu, S., Cai, Y., Zhu, E., Jia, Y., Ji, C., Tang, Z., Fang, J., Feng, X., 2022. Plant-derived lipids play a crucial role in forest soil carbon accumulation. Soil Biol. Biochem. 168, 108645 https://doi.org/10.1016/j.soilbio.2022.108645.

Deng, L., Liu, G.b., Shangguan, Z.p., 2014. Land-use conversion and changing soil carbon stocks in China's 'Grain-for-Green' program: a synthesis. Glob. Chang. Biol. 20, 3544–3556. https://doi.org/10.1111/gcb.12508.

Deng, L., Wang, G.-l., Liu, G.-b., Shangguan, Z.-p, 2016. Effects of age and land-use changes on soil carbon and nitrogen sequestrations following cropland abandonment on the Loess Plateau, China. Ecol. Eng. 90, 105–112. https://doi.org/10.1016/j.ecoleng.2016.01.086.

Deng, L., Liu, S., Kim, D.G., Peng, C., Sweeney, S., Shangguan, Z., 2017. Past and future carbon sequestration benefits of China's grain for green program. Glob. Environ. Chang. 47, 13–20. https://doi.org/10.1016/j.gloenvcha.2017.09.006.

Dong, L., Fan, J., Li, J., Zhang, Y., Liu, Y., Wu, J., Li, A., Shangguan, Z., Deng, L., 2022. Forests have a higher soil C sequestration benefit due to lower C mineralization efficiency: evidence from the central loess plateau case. Agric. Ecosyst. Environ. 339, 108144 https://doi.org/10.1016/j.agee.2022.108144.

Feng, X., Simpson, M.J., 2007. The distribution and degradation of biomarkers in Alberta grassland soil profiles. Org. Geochem. 38, 1558–1570. https://doi.org/10.1016/j.orggeochem.2007.05.001.

Friedlingstein, P., O'sullivan, M., Jones, M.W., Andrew, R.M., Hauck, J., Olsen, A., Peters, G.P., Peters, W., Pongratz, J., Sitch, S., 2020. Global carbon budget 2020. Earth Syst. Sci. Data 12, 3269–3340. https://doi.org/10.5194/essd-12-3269-2020.

Fu, B., Wang, S., Liu, Y., Liu, J., Liang, W., Miao, C., 2017. Hydrogeomorphic ecosystem responses to natural and anthropogenic changes in the Loess Plateau of China. Annu. Rev. Earth Planet. Sci. 45, 223–243. https://doi.org/10.1146/annurev-earth-063016-020552.

Gill, R., Burke, I.C., Milchunas, D.G., Lauenroth, W.K., 1999. Relationship between root biomass and soil organic matter pools in the shortgrass steppe of eastern Colorado. Ecosystems 2, 226–236. https://doi.org/10.1007/s100219900070.

He, M., Fang, K., Chen, L., Feng, X., Qin, S., Kou, D., He, H., Liang, C., Yang, Y., 2021. Depth-dependent drivers of soil microbial necromass carbon across Tibetan alpine grasslands. Glob. Chang. Biol. 28, 936–949. https://doi.org/10.1111/gcb.15969.

IPCC, 2021. Summary for policymakers. In: Climate Change 2021: The Physical Science Basis. Intergovernmental Panel on Climate Change.

Jia, Y., Zhai, G., Zhu, S., Liu, X., Schmid, B., Wang, Z., Ma, K., Feng, X., 2021. Plant and microbial pathways driving plant diversity effects on soil carbon accumulation in subtropical forest. Soil Biol. Biochem. 161, 108375 https://doi.org/10.1016/j.soilbio.2021.108375.

Kögel-Knabner, I., 2002. The macromolecular organic composition of plant and microbial residues as inputs to soil organic matter. Soil Biol. Biochem. 34, 139–162. https://doi.org/10.1016/S0038-0717(01)00158-4.

Lal, R., 2004a. Soil carbon sequestration impacts on global climate change and food security. Science 304, 1623–1627. https://doi.org/10.1126/science.1097396.

Lal, R., 2004b. Soil carbon sequestration to mitigate climate change. Geoderma 123, 1–22. https://doi.org/10.1016/j.geoderma.2004.01.032.

Lan, X., Shan, J., Huang, Y., Liu, X., Lv, Z., Ji, J., Hou, H., Xia, W., Liu, Y., 2022. Effects of long-term manure substitution regimes on soil organic carbon composition in a red paddy soil of southern China. Soil Tillage Res. 221, 105395 https://doi.org/10.1016/j.still.2022.105395.

Lavallee, J.M., Soong, J.L., Cotrufo, M.F., 2019. Conceptualizing soil organic matter into particulate and mineral-associated forms to address global change in the 21st century. Glob. Chang. Biol. 26, 261–273. https://doi.org/10.1111/gcb.14859.

Lehmann, J., Kleber, M., 2015. The contentious nature of soil organic matter. Nature 528, 60–68. https://doi.org/10.1038/nature16069.

Li, J., Zhang, X., Luo, J., Lindsey, S., Zhou, F., Xie, H., Li, Y., Zhu, P., Wang, L., Shi, Y., 2020. Differential accumulation of microbial necromass and plant lignin in synthetic versus organic fertilizer-amended soil. Soil Biol. Biochem. 149, 107967 https://doi.org/10.1016/j.soilbio.2020.107967.

Li, J., Shangguan, Z., Deng, L., 2022a. Free particulate organic carbon plays critical roles in carbon accumulations during grassland succession since grazing exclusion. Soil Tillage Res. 220, 105380 https://doi.org/10.1016/j.still.2022.105380.

Li, N., Xu, Y.-Z., Han, X.-Z., He, H.-B., Zhang, X.-d, Zhang, B., 2015. Fungi contribute more than bacteria to soil organic matter through necromass accumulation under different agricultural practices during the early pedogenesis of a Mollisol. Eur. J. Soil Biol. 67, 51–58. https://doi.org/10.1016/j.ejsobi.2015.02.002.

Li, T., Yuan, Y., Mou, Z., Li, Y., Kuang, L., Zhang, J., Wu, W., Wang, F., Wang, J., Lambers, H., Sardans, J., Penuelas, J., Ren, H., Liu, Z., 2022b. Faster accumulation and greater contribution of glomalin to the soil organic carbon pool than amino sugars do under tropical coastal forest restoration. Glob. Chang. Biol. 29 (2), 533–546. https://doi.org/10.1111/gcb.16467.

Li, T., Cheng, H., Li, Y., Mou, Z., Zhu, X., Wu, W., Zhang, J., Kuang, L., Wang, J., Hui, D., 2023. Divergent accumulation of amino sugars and lignins mediated by soil functional carbon pools under tropical forest conversion. Sci. Total Environ. 881, 163204 https://doi.org/10.1016/j.scitotenv.2023.163204.

Li, X., Huang, J., Qu, C., Chen, W., Chen, C., Cai, P., Huang, Q., 2022c. Diverse regulations on the accumulation of fungal and bacterial necromass in cropland soils. Geoderma 410, 115675. https://doi.org/10.1016/j.geoderma.2021.115675.

Liang, C., 2020. Soil microbial carbon pump: mechanism and appraisal. Soil Ecol. Lett. 2, 241–254. https://doi.org/10.1007/s42832-020-0052-4.

Liang, C., Schimel, J.P., Jastrow, J.D., 2017. The importance of anabolism in microbial control over soil carbon storage. Nat. Microbiol. 2, 17105. https://doi.org/10.1038/nmicrobiol.2017.105.

Liang, C., Amelung, W., Lehmann, J., Kästner, M., 2019. Quantitative assessment of microbial necromass contribution to soil organic matter. Glob. Chang. Biol. 25, 3578–3590. https://doi.org/10.1111/gcb.14781.

Liao, C., Men, X., Wang, C., Chen, R., Cheng, X., 2022. Nitrogen availability and mineral particles contributed fungal necromass to the newly formed stable carbon pool in the alpine areas of Southwest China. Soil Biol. Biochem. 173, 108788 https://doi.org/10.1016/j.soilbio.2022.108788.

Liu, J., Yang, Z., Dang, P., Zhu, H., Gao, Y., Ha, V.N., Zhao, Z., 2017. Response of soil microbial community dynamics to Robinia pseudoacacia L. afforestation in the loess plateau: a chronosequence approach. Plant Soil 423, 327–338. https://doi.org/10.1007/s11104-017-3516-2.

Liu, J., Dang, P., Gao, Y., Zhu, H., Zhu, H., Zhao, F., Zhao, Z., 2018. Effects of tree species and soil properties on the composition and diversity of the soil bacterial community following afforestation. For. Ecol. Manag. 427, 342–349. https://doi.org/10.1016/j.foreco.2018.06.017.

Liu, J., Wang, Q., Ku, Y., Zhang, W., Zhu, H., Zhao, Z., 2022a. Precipitation and soil pH drive the soil microbial spatial patterns in the Robinia pseudoacacia forests at the regional scale. Catena 212, 106120. https://doi.org/10.1016/j.catena.2022.106120.

Liu, L., Gunina, A., Zhang, F., Cui, Z., Tian, J., 2022b. Fungal necromass increases soil aggregation and organic matter chemical stability under improved cropland management and natural restoration. Sci. Total Environ. 858, 159953 https://doi.org/10.1016/j.scitotenv.2022.159953.

Liu, Y., Fang, Y., An, S., 2020. How C: N: P stoichiometry in soils and plants responds to succession in Robinia pseudoacacia forests on the Loess Plateau, China. For. Ecol. Manag. 475, 118394 https://doi.org/10.1016/j.foreco.2020.118394.

Luo, R., Kuzyakov, Y., Zhu, B., Qiang, W., Zhang, Y., Pang, X., 2022. Phosphorus addition decreases plant lignin but increases microbial necromass contribution to soil organic carbon in a subalpine forest. Glob. Chang. Biol. 28, 4194–4210. https://doi.org/10.1111/gcb.16205.

Ma, S., Zhu, B., Chen, G., Ni, X., Zhou, L., Su, H., Cai, Q., Chen, X., Zhu, J., Ji, C., 2022. Loss of soil microbial residue carbon by converting a tropical forest to tea plantation. Sci. Total Environ. 818, 151742 https://doi.org/10.1016/j.scitotenv.2021.151742.

Ma, T., Zhu, S., Wang, Z., Chen, D., Dai, G., Feng, B., Su, X., Hu, H., Li, K., Han, W., 2018. Divergent accumulation of microbial necromass and plant lignin components in grassland soils. Nat. Commun. 9, 1–9. https://doi.org/10.1038/s41467-018-05891-1.

Man, M., Wagner-Riddle, C., Dunfield, K.E., Deen, B., Simpson, M.J., 2021. Long-term crop rotation and different tillage practices alter soil organic matter composition and degradation. Soil Tillage Res. 209, 104960 https://doi.org/10.1016/j.still.2021.104960.

Mo, X., Wang, M., Wang, Y., Chen, X., Zhang, A., Zeng, H., Zheng, Y., Kong, D., Wang, J., 2022. Molecular-level characteristics of soil organic carbon in rhizosheaths from a semiarid grassland of North China. Soil Biol. Biochem. 170, 108682 https://doi.org/10.1016/j.soilbio.2022.108682.

Mou, Z., Kuang, L., He, L., Zhang, J., Zhang, X., Hui, D., Li, Y., Wu, W., Mei, Q., He, X., Kuang, Y., Wang, J., Wang, Y., Lambers, H., Sardans, J., Peñuelas, J., Liu, Z., 2021. Climatic and edaphic controls over the elevational pattern of microbial necromass in subtropical forests. Catena 207, 105707. https://doi.org/10.1016/j.catena.2021.105707.

Mustafa, A., Frouz, J., Naveed, M., Ping, Z., Nan, S., Minggang, X., Núñez-Delgado, A., 2022. Stability of soil organic carbon under long-term fertilization: results from $^{13}C$ NMR analysis and laboratory incubation. Environ. Res. 205, 112476 https://doi.org/10.1016/j.envres.2021.112476.

Newcomb, C.J., Qafoku, N.P., Grate, J.W., Bailey, V.L., De Yoreo, J.J., 2017. Developing a molecular picture of soil organic matter–mineral interactions by quantifying organo–mineral binding. Nat. Commun. 8, 1–8. https://doi.org/10.1038/s41467-017-00407-9.

Saiya-Cork, K., Sinsabaugh, R., Zak, D., 2002. The effects of long term nitrogen deposition on extracellular enzyme activity in an Acer saccharum forest soil. Soil Biol. Biochem. 34, 1309–1315. https://doi.org/10.1016/S0038-0717(02)00074-3.

Shao, P., Liang, C., Lynch, L., Xie, H., Bao, X., 2019. Reforestation accelerates soil organic carbon accumulation: evidence from microbial biomarkers. Soil Biol. Biochem. 131, 182–190. https://doi.org/10.1016/j.soilbio.2019.01.012.

Shao, P., Lynch, L., Xie, H., Bao, X., Liang, C., 2021. Tradeoffs among microbial life history strategies influence the fate of microbial residues in subtropical forest soils. Soil Biol. Biochem. 153, 108112 https://doi.org/10.1016/j.soilbio.2020.108112.

Silva-Sánchez, A., Soares, M., Rousk, J., 2019. Testing the dependence of microbial growth and carbon use efficiency on nitrogen availability, pH, and organic matter quality. Soil Biol. Biochem. 134, 25–35. https://doi.org/10.1016/j.soilbio.2019.03.008.

Six, J., Frey, S., Thiet, R., Batten, K., 2006. Bacterial and fungal contributions to carbon sequestration in agroecosystems. Soil Sci. Soc. Am. J. 70, 555–569. https://doi.org/10.2136/sssaj2004.0347.

Sokol, N.W., Sanderman, J., Bradford, M.A., 2018. Pathways of mineral-associated soil organic matter formation: integrating the role of plant carbon source, chemistry, and point of entry. Glob. Chang. Biol. 25, 12–24. https://doi.org/10.1111/gcb.14482.

Su, Z., Su, B., Wu, Y., Zhang, Y., Wang, J., Chen, Y., Shangguan, Z., 2023. A less complex but more specialized microbial network resulted in faster fine-root decomposition in young stands of Robinia pseudoacacia. Appl. Soil Ecol. 182, 104735 https://doi.org/10.1016/j.apsoil.2022.104735.

Thevenot, M., Dignac, M.-F., Rumpel, C., 2010. Fate of lignins in soils: a review. Soil Biol. Biochem. 42, 1200–1211. https://doi.org/10.1016/j.soilbio.2010.03.017.

Vance, E.D., Brookes, P.C., Jenkinson, D.S., 1987. An extraction method for measuring soil microbial biomass C. Soil Biol. Biochem. 19, 703–707. https://doi.org/10.1016/0038-0717(87)90052-6.

Wang, B., An, S., Liang, C., Liu, Y., Kuzyakov, Y., 2021a. Microbial necromass as the source of soil organic carbon in global ecosystems. Soil Biol. Biochem. 162, 108422 https://doi.org/10.1016/j.soilbio.2021.108422.

Wang, B., Liang, C., Yao, H., Yang, E., An, S., 2021b. The accumulation of microbial necromass carbon from litter to mineral soil and its contribution to soil organic

carbon sequestration. Catena 207, 105622. https://doi.org/10.1016/j.catena.2021.105622.
Wang, B., Huang, Y., Li, N., Yao, H., Yang, E., Soromotin, A.V., Kuzyakov, Y., Cheptsov, V., Yang, Y., An, S., 2022a. Initial soil formation by biocrusts: nitrogen demand and clay protection control microbial necromass accrual and recycling. Soil Biol. Biochem. 167, 108607 https://doi.org/10.1016/j.soilbio.2022.108607.
Wang, Q.-C., Yang, L.-M., Song, G., Jin, S.-S., Hu, H.-W., Wu, F., Zheng, Y., He, J.-Z., 2022b. The accumulation of microbial residues and plant lignin phenols are more influenced by fertilization in young than mature subtropical forests. For. Ecol. Manag. 509, 120074 https://doi.org/10.1016/j.foreco.2022.120074.
Wang, W., Zhang, Q., Sun, X., Chen, D., Insam, H., Koide, R.T., Zhang, S., 2020. Effects of mixed-species litter on bacterial and fungal lignocellulose degradation functions during litter decomposition. Soil Biol. Biochem. 141, 107690 https://doi.org/10.1016/j.soilbio.2019.107690.
Whalen, E.D., Grandy, A.S., Sokol, N.W., Keiluweit, M., Ernakovich, J., Smith, R.G., Frey, S.D., 2022. Clarifying the evidence for microbial- and plant-derived soil organic matter, and the path toward a more quantitative understanding. Glob. Chang. Biol. 28 (24), 7167–7185. https://doi.org/10.1111/gcb.16413.
Wu, J., Liang, G., Hui, D., Deng, Q., Xiong, X., Qiu, Q., Liu, J., Chu, G., Zhou, G., Zhang, D., 2016. Prolonged acid rain facilitates soil organic carbon accumulation in a mature forest in Southern China. Sci. Total Environ. 544, 94–102. https://doi.org/10.1016/j.scitotenv.2015.11.025.
Yang, L., Wang, J., Geng, Y., Niu, S., Tian, D., Yan, T., Liu, W., Pan, J., Zhao, X., Zhang, C., 2022a. Heavy thinning reduces soil organic carbon: evidence from a 9-year thinning experiment in a pine plantation. Catena 211, 106013. https://doi.org/10.1016/j.catena.2021.106013.
Yang, W., Zhang, D., Cai, X., Yang, X., Zhang, H., Wang, Y., Diao, L., Luo, Y., Cheng, X., 2023. Natural revegetation over ~160 years alters carbon and nitrogen sequestration and stabilization in soil organic matter on the Loess Plateau of China. Catena 220, 106647. https://doi.org/10.1016/j.catena.2022.106647.
Yang, Y., Dou, Y., Wang, B., Wang, Y., Liang, C., An, S., Soromotin, A., Kuzyakov, Y., 2022b. Increasing contribution of microbial residues to soil organic carbon in grassland restoration chronosequence. Soil Biol. Biochem. 170, 108688 https://doi.org/10.1016/j.soilbio.2022.108688.
Yu, W., Huang, W., Weintraub-Leff, S.R., Hall, S.J., 2022. Where and why do particulate organic matter (POM) and mineral-associated organic matter (MAOM) differ among diverse soils? Soil Biol. Biochem. 172, 108756 https://doi.org/10.1016/j.soilbio.2022.108756.
Yuan, H., Zhu, Z., Liu, S., Ge, T., Jing, H., Li, B., Liu, Q., Lynn, T.M., Wu, J., Kuzyakov, Y., 2016. Microbial utilization of rice root exudates: $^{13}$C labeling and PLFA composition. Biol. Fertil. Soils 52, 615–627. https://doi.org/10.1007/s00374-016-1101-0.
Zhang, W., Xu, Y., Gao, D., Wang, X., Liu, W., Deng, J., Han, X., Yang, G., Feng, Y., Ren, G., 2019. Ecoenzymatic stoichiometry and nutrient dynamics along a revegetation chronosequence in the soils of abandoned land and Robinia pseudoacacia plantation on the Loess Plateau, China. Soil Biol. Biochem. 134, 1–14. https://doi.org/10.1016/j.soilbio.2019.03.017.
Zhang, X., Amelung, W., 1996. Gas chromatographic determination of muramic acid, glucosamine, mannosamine, and galactosamine in soils. Soil Biol. Biochem. 28, 1201–1206. https://doi.org/10.1016/0038-0717(96)00117-4.
Zhao, X., Tian, P., Liu, S., Yin, P., Sun, Z., Wang, Q., 2022. Mean annual temperature and carbon availability respectively controlled the contributions of bacterial and fungal residues to organic carbon accumulation in topsoil across China's forests. Glob. Ecol. Biogeogr. 32 (1), 120–131. https://doi.org/10.1111/geb.13605.
Zhong, Y., Yan, W., Wang, R., Shangguan, Z., 2017. Differential responses of litter decomposition to nutrient addition and soil water availability with long-term vegetation recovery. Biol. Fertil. Soils 53, 939–949. https://doi.org/10.1007/s00374-017-1242-9.
Zhu, X., Jackson, R.D., DeLucia, E.H., Tiedje, J.M., Liang, C., 2020. The soil microbial carbon pump: from conceptual insights to empirical assessments. Glob. Chang. Biol. 26, 6032–6039. https://doi.org/10.1111/gcb.15319.